JMEPEG (2012) 21:1956–1961
DOI: 10.1007/s11665-011-0101-3

1059-9495/$19.00

# Tobacco Stem-Based Activated Carbons for High Performance Supercapacitors

*Xiaohong Xia, Hongbo Liu, Lei Shi, and Yuede He*

*(Submitted December 9, 2010; in revised form December 11, 2011)*

**Tobacco stem-based activated carbons (TS-ACs) were prepared by simple KOH activation and their application as electrodes in the electrical double layer capacitor (EDLC) performed successfully. The BET surface area, pore volume, and pore size distribution of the TS-ACs were evaluated based on $N_2$ adsorption isotherms at 77 K. The surface area of the obtained activated carbons varies over a wide range (1472.8-3326.7 $m^2/g$) and the mesoporosity was enhanced significantly as the ratio of KOH to tobacco stem (TS) increased. The electrochemical behaviors of series TS-ACs were characterized by means of galvanostatic charging/discharging, cyclic voltammetry, and impedance spectroscopy. The correlation between electrochemical properties and pore structure was investigated. A high specific capacitance value as 190 F/g at 1 $mA/cm^2$ was obtained in 1 M $LiPF_6$-EC/DMC/DEC electrolyte solution. Furthermore, good performance is also achieved even at high current densities. A development of new use for TS into a valuable energy storage material is explored.**

**Keywords** activated carbon, electrochemical performance, KOH activation, tobacco stem

## 1. Introduction

Electric double layer capacitors (EDLC) with both high energy density and power density have been strongly recommended especially from the viewpoint of their application to auxiliary power sources of hybrid electric vehicles or fuel cell electric vehicles. Activated carbon is a feasible material for the storage of energy due to its unique surface characteristics, stable physicochemical properties, good conductivity, low cost and availability (Ref 1). In general, the larger the surface area of the activated carbon sample, the higher is the capacitance. However a nonlinear relationship has been definitely observed between the surface area and the specific capacitance (Ref 2), in respect that some other parameters of activated carbon such as pore geometry, pore size, pore size distribution, surface functional groups, and size of the electrolyte ions also have great influence on the EDLC performance (Ref 3, 4). For the purpose of high density and power applications, besides high surface area, a reasonable proportion of mesopores (i.e., 2 nm < pore diameter < 50 nm) within ACs is also demanded as a key factor determining the capacitive performances of EDLCs in considering the free movement of solvated ions and the establishment of a complete array for the electric double layers. Mesoporous carbon with uniform pore size were widely synthesized using different kinds of templates including hard template (mesoporous silica) (Ref 5, 6) or/and soft template (block copolymer) (Ref 7, 8). However, not only the procedure involved was complicated but also the surface area of the resulting porous carbon was relatively low for the application in EDLCs. Hence, various activation methods were investigated to develop porous structures of ACs (Ref 9, 10), which aimed at increasing power and energy density as well as lowering fabrication costs while using environmentally friendly materials.

Recently, as a renewable source, biomasses have attracted much attention for their promising applications in the preparation of activated carbons. A large number of studies have been devoted to the production of activated carbons from biomass, such as cornstalks (Ref 9), durian shell (Ref 11), cherry stone (Ref 12), corn grains (Ref 13), etc. It has been already extensively demonstrated that the pore properties of activated carbons depend not only on the experimental conditions of the carbonization and activation steps but also preponderantly on the original nature and structure of the involved precursor.

Tobacco is a kind of important economic crop. According to a statistic in the year 2008 of China, the amount of the tobacco waste discharge including tobacco stems (TSs) reached about 1.2-1.5 million tons. Unfortunately, the treatment of tobacco waste in China at present is directly buried or burned off, which would bring about serious environmental problems. So, it is urgent to explore multipurpose utilization technologies to dispose tobacco waste. TSs contain rich carbon species and the major components of it are cellulose, hemicellulose, and lignin, which can also act as a suitable precursor for the formation of porous activated carbons (Ref 14). Herein, we report a simple, cheap, and high yield strategy for the preparation of activated carbons with high surface area and mesoporosity from TSs, and their electrochemical performance in EDLCs was thoroughly investigated in nonaqueous electrolyte for the first time.

## 2. Experimental

### 2.1 Preparation of TS-ACs

Activated carbons were prepared by KOH activation utilizing TSs as the starting material. The raw TSs were first

**Xiaohong Xia, Hongbo Liu, Lei Shi,** and **Yuede He,** College of Materials Science and Engineering, Hunan University, Changsha 410082 Hunan, China. Contact e-mail: xia_spring@163.com.

washed, dried at 120 °C overnight, and crushed into powder. The powder was then heated at 600 °C for 2 h in an atmosphere of $N_2$. At this step, a carbonized product (CP) was formed. After carbonization treatment, the CP samples were activated with KOH at different mass ratio in $N_2$ atmosphere at 900 °C for 1 h and washed with distilled water and then treated with dilute HCl solution. Finally, the carbon material was further washed with distilled water until the pH value of the system reached about 7.0, and then dried at 120 °C overnight. The TSs activated with various KOH dosages (mass ratios of 1:1, 2:1, 2.5:1, 3.0:1, 4.0:1 (KOH/CP)) are denoted as TS-AC 1-5.

### 2.2 Analysis of the Porous Structure and the Chemical Characteristics of TS-ACs

Pyrolysis process was described by TG and DTG curves, determined during thermal analysis of TSs in helium stream using thermal balance STA409 PC Luxx (NETZSCH Instruments Corp., Tirschenreuth, Germany) in thermal conditions adequate for a chamber reactor.

Surface area and pore structure of the TS-ACs samples were characterized with auto-adsorption apparatus ASAP 2020 Surface Area & Pore-Size Analyzer (Micromeritics Corp., Norcross, USA) by adsorption/desorption of nitrogen at 77 K. The apparent surface area was determined by the Brunauer, Emmett, and Teller (BET) equation from the $N_2$ adsorption isotherm. The total pore volumes, $V_t$ (from the last point of isotherm at relative pressure equal to 0.99) and pore size distribution were calculated using density functional theory (DFT).

### 2.3 Electrochemical Measurements

The fabrication of carbon electrodes was as follows: Activated carbons (active material), carbon black (conductivity enhancing material), and PTFE (60 wt.% solution, binder) were mixed in a mass ratio of 90:5:5 and dispersed in distilled water (the mass ratio of carbon to water was set as 1:2). After homogenized in a mortar, the slurry was rolled into a thin film of uniform thickness ($0.5 \pm 0.1$ mm). From this film, 12 mm circular electrodes were punched out and pressed onto a stainless steel mesh (as a current collector). The carbon-coated stainless steel mesh was then dried under vacuum at 120 °C for ca. 12 h. Test capacitors were constructed in a glove box. A separator Celgard 3400 soaked with nonaqueous electrolyte solution (1 M $LiPF_6$-EC/DMC/DEC (1:1:1 V)) was sandwiched between two identical carbon electrodes in a button cell.

Electrochemical measurements (CV, EIS) were performed on an electrochemical workstation CHI660A (Chenhua Instrument Corp., Shanghai, China) at room temperature, using two-electrode electrochemical capacitor cells. Cyclic voltammograms were recorded from 0 to 2.7 V at various sweep rates and the Nyquist plots were recorded potentiostatically (0 V) by applying an alternating voltage of 5 mV amplitude in the 100 kHz-1 mHz frequency range. The constant-current discharge-charge tests were conducted in the voltage range of 0-2.7 V with a Battery Tester (Wuhan Jinnuo Co., Wuhan, China) at current densities of 1-50 mA/cm$^2$.

## 3. Results and Discussion

### 3.1 Thermo-gravimetric Analysis

Figure 1 depicts the thermograms of TS. The curve showed an analogous weight decrease as other biomass materials during heat-treatment (Ref 15). The weight loss around 100 °C is attributed to loss of superficial moisture from TSs. A major weight loss can be observed between 250 and 500 °C and reaches the maximum at ca. 315 °C, which can be attributed to decomposition of cellulose, hemicellulose, and lignin in TSs to yield low-volatile organics. The pyrolytic processes result in carbonization and attendant aromatic condensation. Further heating to the temperature of ca. 600 °C slows down pyrolytic processes at a negligible and decreasing weight loss—it indicates that a gradual restructuring of carbon proceeds. The carbon yield is about 30% after heating to 900 °C.

### 3.2 Porous Texture Characterization

Nitrogen adsorption/desorption isotherms at 77 K of TS-ACs prepared with different ratios of KOH/CP are described in Fig. 2. The isotherm morphology of TS-ACs varies remarkably with the increase of KOH/CP ratio. TS-AC 1, TS-AC 2, and TS-AC 3 all exhibit Type I adsorption isotherms characteristic of microporous carbons, but a wider knee was illustrated, indicating the development of a wider micropores. Different from TS-AC 1-3, the shapes of the isotherms for TS-AC 4 and TS-AC 5 are a mixture of type I and type IV isotherms and show obvious capillary condensation step (hysteresis loops) at medium relative

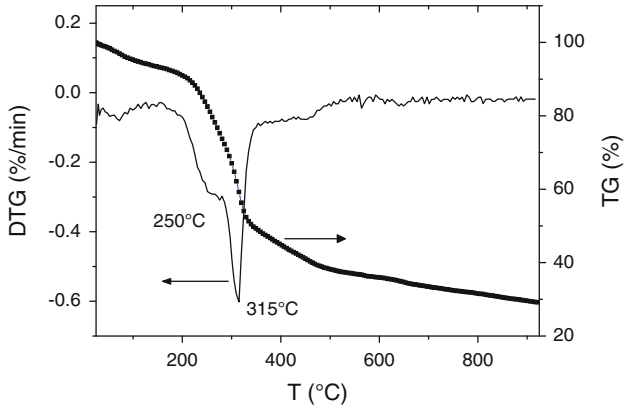


**Fig. 1** Thermo-gravimetric analysis for TSs (5 °C/min in nitrogen atmosphere)

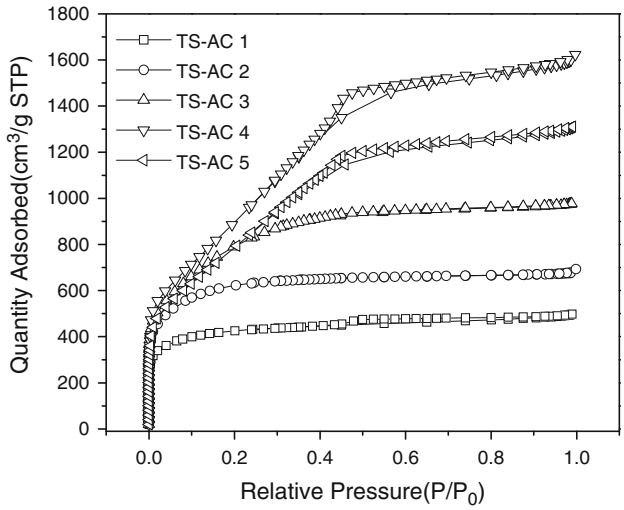


**Fig. 2** $N_2$ sorption isotherms of TS-ACs series samples

pressure, indicating that besides micropores, a considerable amount of mesopores were created.

The specific surface areas and pore structural parameters of TS-ACs are summarized in Table 1. The specific surface area and total pore volume increase first and then decrease as the ratio of KOH/CP changing from 1.0 to 4.0. It is suggested that during the activation, the activating agent KOH reacts with the reactive centers of the carbonized material, such as disorganized carbons, carbons with heteroatoms, and carbons on graphene edges, creating new pores and widening the existing ones. The activation of carbon with KOH proceeds as $6KOH + C \leftrightarrow 2\ K + 3H_2 + 2K_2CO_3$, followed by decomposition of $K_2CO_3$ and/or reaction of $K/K_2CO_3/CO_2$ with carbon (Ref 16). When the ratio of the KOH/CP is 3, the surface area total, pore volume, and mesoporosity reach the highest values, being 3326.7 $m^2/g$, 2.443 $cm^3/g$, and 65.7%, respectively, but further increasing the ratio to 4 results in slight decreases of porosity of the carbon sample. This is because that the activating agent not only develops the porosity but also damages the structures of the pores at too high a concentration.

Figure 3 presents the pore size distribution of TS-ACs calculated by DFT method, which consist well with the results of the adsorption/desorption isotherms in Fig. 2. Combined with Table 1, we found that when the ratio of the KOH/CP increases, the volumes in pores of sizes between 1-2 and 2-5 nm increased remarkably, which means pores were widened and mesopores can be effectively created by corrosion of KOH on the micropore wall of TS-ACs due to a relative weak carbon skeleton derived from TSs like other biomasses (Ref 17). This would be benefit for ion quick transport especially in organic electrolyte. However, as the KOH/CP ratio was increased up to 4.0, the over-activation of KOH brought about the collapsing of mesopore wall and the corresponding surface area subsequently shrank and there is a balance between mesopore creation and collapsing during activation process.

### 3.3 Electrochemical Characterizations

**3.3.1 Cyclic Voltammetry Behavior of TS-ACs Electrode.** The voltammograms of electrochemical capacitor cells with the TS-ACs as electrodes are presented in Fig. 4 at different scan rates in 1 M $LiPF_6$-EC/DMC/DEC (1:1:1 V) nonaqueous solution. At low scan rates, all the samples showed quite rectangular curve shape without observation of obvious oxygen and hydrogen evolution peaks, suggesting a typical nonfaradic adsorption/desorption reaction within the potential range (0-2.7 V) employed. But their voltammogram shapes become gradually distorted as elevated scan rates. The distorted rectangle may be due to diffusion-limited capacitance, which may in true be ascribed to electrolyte trapped in the micropores of the carbons (Ref 18). For comparison, the cyclic voltammetric performance of varies TS-ACs samples were also conducted (see Fig. 5), the scan rate was set at 50 mV/s. The five TS-ACs samples exhibit distinguish behavior from each other, with TS-AC 4 retaining the most rectangular CV profile and exhibiting the highest specific capacitance. The nearly 90° change in the CV curves of TS-AC 4 and TS-AC 5 at the switching potential suggested that they had smaller equivalent series resistance (ESR) as an ideal capacitor desired, which can be attributed to a quick kinetic process for the diffusion of ions resulting from their relative high mesoporosity (shown in Fig. 3). The micropores play an essential role for ion adsorption, whereas the mesopores are necessary for their quick transport to the bulk of the materials.

**3.3.2 Charge-Discharge Behavior of TS-ACs Electrode.** The capacitances of as-prepared TS-ACs at different current densities were demonstrated in Fig. 6. The specific capacitances of all samples decreases with discharge current, confirming that at the low currents the ions have enough time to diffuse into the micropores of carbons, while at the high currents the ions can only partially penetrate into the micropores due to the steric limitations. However, different from other samples, the specific capacitances of TS-AC 4 and TS-AC 5 drop rapidly at low discharge current and then become stable

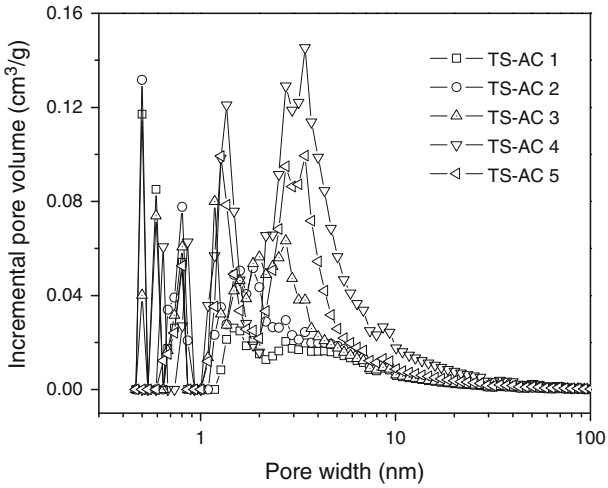


**Fig. 3** Pore size distribution of TS-ACs samples calculated by DFT method

**Table 1 The specific surface area and pore structures of TS-ACs samples**

| Samples | $S_{BET}$, $m^2/g$ | $S_{micro}$[a], $m^2/g$ | $S_{meso}$[a], $m^2/g$ | $V_{<1nm}$[a], $cm^3/g$ | $V_{micro}$[a], $cm^3/g$ | $V_{meso}$[a], $cm^3/g$ | $V_{tot}$[a], $cm^3/g$ | $V_{meso}/V_{tot}$, % | $D$[b], nm |
|---|---|---|---|---|---|---|---|---|---|
| TS-AC 1 | 1472.8 | 1272.4 | 191.1 | 0.216 | 0.638 | 0.122 | 0.760 | 16.1 | 2.06 |
| TS-AC 2 | 2187.5 | 2030.7 | 167.8 | 0.205 | 0.841 | 0.193 | 1.034 | 18.7 | 1.89 |
| TS-AC 3 | 2868.6 | 2159.5 | 632.8 | 0.192 | 0.883 | 0.625 | 1.508 | 41.4 | 2.10 |
| TS-AC 4 | 3326.7 | 1948.8 | 1365.3 | 0.092 | 0.836 | 1.607 | 2.443 | 65.7 | 2.94 |
| TS-AC 5 | 2912.5 | 1978.6 | 956.3 | 0.130 | 0.819 | 1.249 | 2.068 | 60.4 | 2.84 |

BET surface area
[a]Calculated using DFT
[b]Average pore diameter: Adsorption average pore width (4 V/A by BET)

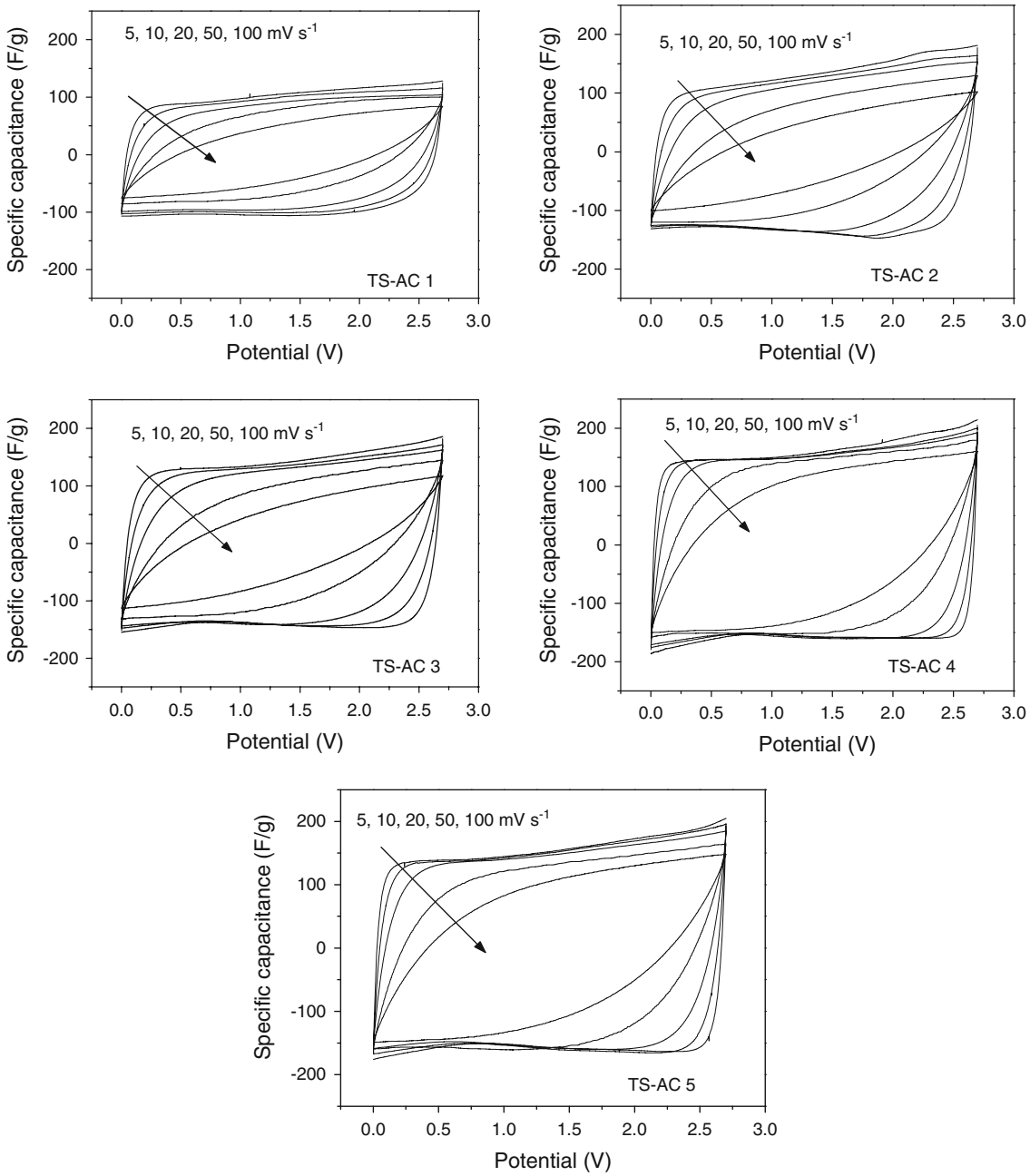


**Fig. 4** Voltammograms of TS-ACs series samples at different scan rates of 5-100 mV/s between 0 and 2.7 V in 1 M $LiPF_6$-EC/DMC/DEC (1:1:1 V) solution

above 10 mA/cm$^2$, which agrees well with their CVs shown in Fig. 4 and 5. The sample TS-AC 4 with both the highest specific surface area and mesoporosity showed the maximum specific capacitance value as 190 F/g at 1 mA/cm$^2$, which is much higher than the result recently reported ($<$140 F/g) (Ref 2) and retained as high as 80% ($\sim$150 F/g) even when the current density was enlarged 50 times. It is widely believed that to obtain high capacitance and rate performance at the same time especially in organic electrolyte, porous carbon with a high specific surface area and a large amount of mesopores is effective. As shown in Table 1, the pore volumes of TS-AC 4 are mainly located in 1-2 and 2-5 nm, which are suitable for adsorption and quick transport of organic electrolytes. There are also other carbons with high mesoporosity. For example, nanoporous carbons were prepared using colloidal crystal as a template (Ref 5). Although the capacitance did not decreased even at a large current density of 10 A/g in organic electrolyte, the capacitance is not ideal enough (120 F/g) due to their relative low specific surface areas of carbon samples ranged from 1089 to 1455 m$^2$/g. To improve the surface area of mesoporous carbon, a combination of self-assembly (F127) and KOH chemical activation was introduced (Ref 19). Superior capacitive performances were showed in aqueous electrolyte of the carbon samples, but unfortunately, capacitive performance in organic electrolyte was not mentioned and the preparation is a multi-step process, and the cost is extremely high.

The Ragone plots are frequently used in demonstration of power densities and energy densities of EDLC as shown in

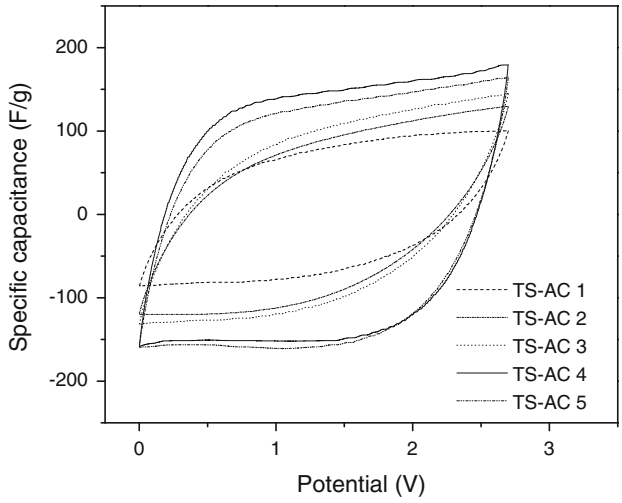


**Fig. 5** Voltammograms of TS-ACs series samples at scan rate of 50 mV/s

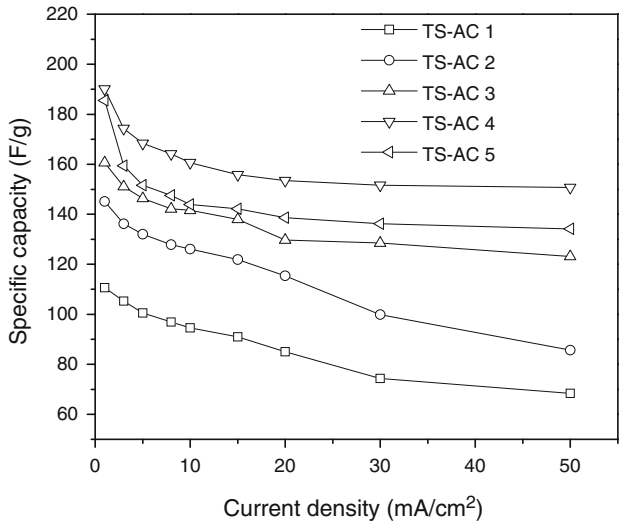


**Fig. 6** The dependence of the capacitance of the TS-ACs series samples on the current density

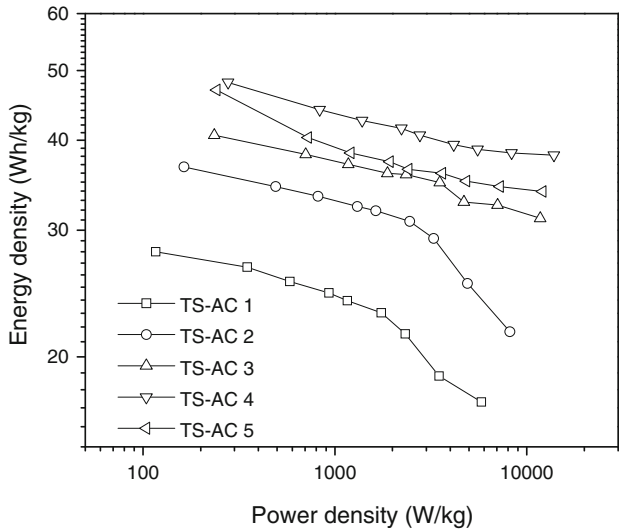


**Fig. 7** Ragone plots of TS-ACs in nonaqueous electrolyte. Power density and energy density are based on the mass of active electrode material, and exclude the mass of the electrolyte, current collectors, and cell packaging

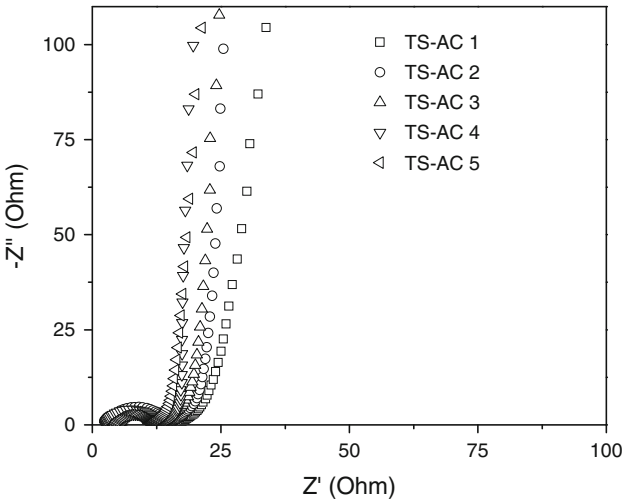


**Fig. 8** Nyquist curves of impedances for TS-ACs

Fig. 7. The highest value as 48.1 Wh/kg at low current density is obtained with TS-AC 4, the carbon with highest specific capacitance. With increasing specific power, the benefit of mesopores in the carbon electrodes are clearly demonstrated by the stable performance of TS-AC 4, which retains 38.3 Wh/kg at 10000 W/kg.

**3.3.3 Impedance Measurements of TS-ACs Electrode.** The impedance spectra in the complex plane (Nyquist plots) of TS-ACs electrodes are shown in Fig. 8. In all the cases, the Nyquist plots exhibit a typical impedance characteristic of EDLC in nonaqueous electrolytes: a depressed semicircle at high frequency region, a 45° line in middle frequency region and a nearly vertical line at low frequency. The very high frequency intercept on the real axis was estimated around 4Ω, which is associated with the resistance mainly arising form the electrolyte (Ref 20). The depressed semicircles represent a parallel combination of resistive and capacitive components and the width of the semicircle is a measure of the resistance due to the diffusion of ions through the carbon pore network (Ref 21). The values decrease in the sequence of TS-AC 1, 2, 3, 4, and 5, which means the larger pore sizes obtained by activation of high KOH ratios increase the connecting channels between pores allowing better ion transport at fast discharge rates (Ref 22). At low frequency, the resistance determined by the intercept that the linear region makes with the real impedance axis represents the overall resistance of the electrochemical cell. The smaller the resistance is, the less the capacitance losses during cycling, especially at a high current density. It can be observed that the resistances decrease in the sequence of TS-AC 1, 2, 3, 5, and 4, which is in good agreement with the results obtained by galvanostatic cycling study as shown in Fig. 6.

In order to further investigate the penetration of the alternating current into the pore system of the electrodes materials and illustrate how much of solvated ions access the pores at a specific frequency, a capacitance versus frequency plot for TS-ACs is shown in Fig. 9. In the high frequency range, there are no significant differences between samples as

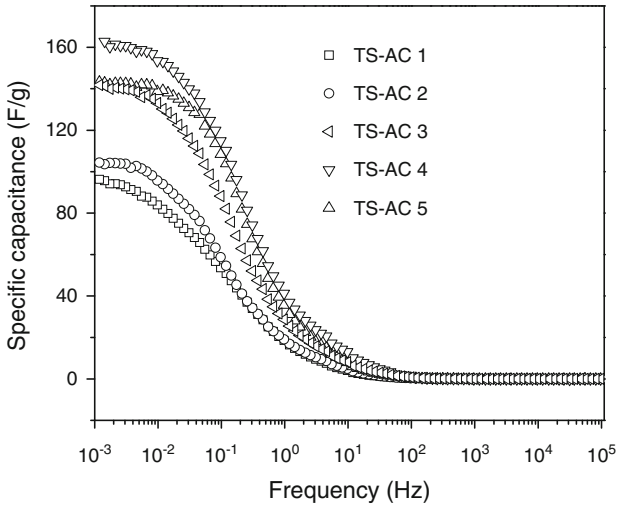


**Fig. 9** Capacitance versus frequency plots for TS-ACs

there is no time for ions access the whole porosity. However, in the low frequency range (from 10 to 1 mHz), nearly a complete penetration of the ions into the pores is allowed and the quite stable values indicate the domination of the capacitive behavior at the electrolyte/carbon interface. The capacitance values of TS-AC 4 and 5 are much higher than other samples and the decrease of their capacitance is shifted to slightly higher frequency, which means their high mesoporosity pore system favors fast diffusion of electrolyte at high frequency. These tow samples can supply capacitance up to 120 F/g at 100 mHz, which is interesting from a practical point of view.

## 4. Conclusions

The potential application of TSs-based activated carbons in EDLCs performance has been confirmed successfully from the results of KOH activated TS-ACs carbons. The TS-based activated carbons possessed higher BET surface area (3326.7 $m^2$/g), larger pore volume (2.443 $cm^3$/g) and higher mesoporostiy (65.7%) than other AC samples. The results of the cyclic voltammogram explored that the samples with high mesoporosity exhibit good performance at high current density. Among all the TS-ACs, the sample TS-AC 4 shows the highest specific capacitance value of 190 F/g and retains 38.3 Wh/kg at 10000 W/kg in nonaqueous electrolyte solution which is much higher than the result recently reported.

### Acknowledgments

The authors would like to thank the financial support from the National Natural Science Foundation of China (No. 50872032) and the Fundamental Research Funds for the Central Universities (No. 531107040185).

### References

1. A.G. Pandolfo and A.F. Hollenkamp, Carbon Properties and Their Role In Supercapacitors, *J. Power Sour.*, 2006, **157**, p 11–27
2. T.E. Rufford, D. Hulicova-Jurcakova, E. Fiset et al., Double-Layer Capacitance of Waste Coffee Ground Activated Carbons in an Organic Electrolyte, *Electrochem. Commun.*, 2009, **11**, p 974–977
3. B.P. Bakhmatyuk, B.Y. Venhryn, I.I. Grygorchak et al., Influence of Chemical Modification of Activated Carbon Surface on Characteristics of Supercapacitors, *J. Power Sour.*, 2008, **180**, p 890–895
4. E.J. Ra, E. Raymundo-Pinero, Y.H. Lee, and F. Beguin, High Power Supercapacitors Using Polyacrylonitrile-Based Carbon Nanofiber Paper, *Carbon*, 2009, **47**, p 2984–2992
5. H. Yamada, I. Moriguchi, and T. Kudo, Electric Double Layer Capacitance on Hierarchical Porous Carbons in an Organic Electrolyte, *J. Power Sour.*, 2008, **175**, p 651–656
6. J.H. Jiang, Q.M. Gao, K.Sh. Xia, and J. Hu, Enhanced Electrical Capacitance of Porous Carbons by Nitrogen Enrichment and Control of the Pore Structure, *Microporous Mesoporous Mater.*, 2009, **118**, p 28–34
7. H.Q. Li, R.L. Liu, D.Y. Zhao, and Y.Y. Xia, Electrochemical Properties of an Ordered Mesoporous Carbon Prepared by Direct Tri-Constituent Co-Assembly, *Carbon*, 2007, **45**, p 2628–2635
8. L.X. Li, H.H. Song, and X.H. Chen, Ordered Mesoporous Carbons from the Carbonization of Sulfuric-Acid-Treated Silica/Triblock Copolymer/Sucrose Composites, *Microporous Mesoporous Mater.*, 2006, **94**, p 9–14
9. F. Zhang, H. Ma, J. Chen et al., Preparation and Gas Storage of High Surface Area Microporous Carbon Derived from Biomass Source Cornstalks, *Bioresour. Technol.*, 2008, **99**, p 4803–4808
10. D. Kalpana, S.H. Cho, S.B. Lee et al., Recycled Waste Paper—A New Source of Raw Material for Electric Double-Layer Capacitors, *J. Power Sour.*, 2009, **190**, p 587–591
11. T.C. Chandra, M.M. Mirna, and J. Sunarso, Activated Carbon from Durian Shell: Preparation and Characterization, *J. Taiwan Inst. Chem. Eng.*, 2009, **40**, p 457–462
12. M. Olivares-Marín, J.A. Fernández, and M.J. Lázaro, Cherry Stones as Precursor of Activated Carbons for Supercapacitors, *Mater. Chem. Phys.*, 2009, **114**, p 323–327
13. M.S. Balathanigaimani, W.G. Shim, M.J. Lee et al., Highly Porous Electrodes from Novel Corn Grains-Based Activated Carbons for Electrical Double Layer Capacitors, *Electrochem. Commun.*, 2008, **10**, p 868–871
14. W. Li, L.B. Zhang, J.H. Peng et al., Preparation of High Surface Area Activated Carbons from Tobacco Stems with $K_2CO_3$ Activation Using Microwave Radiation, *Ind. Crop Prod.*, 2008, **27**, p 341–347
15. B. Cagnon, X. Py, A. Guillot et al., Contributions of Hemicellulose, Cellulose and Lignin to the Mass and the Porous Properties of Chars and Steam Activated Carbons from Various Lignocellulosic Precursors, *Bioresour. Technol.*, 2009, **100**, p 292–298
16. Y.W. Zhu, S. Muraali, M.D. Stoller et al., Carbon-based Supercapacitors Produced by Activation of Graphene, *Science*, 2011, **332**, p 1537–1541
17. M.S. Balathanigaimani, W.-G. Shim, C. Kim et al., Surface Structural Characterization of Highly Porous Activated Carbon Prepared from Corn Grain, *Surf Interface Anal.*, 2009, **41**, p 484–488
18. M.R. Jisha, Y.J. Hwang, J.S. Shin et al., Electrochemical Characterization of Supercapacitors Based on Carbons Derived from Coffee Shells, *Mater. Chem. Phys.*, 2009, **115**, p 33–39
19. W. Xing, C.C. Huang, and S.P. Zhuo, Hierarchical Porous Carbons with High Performance for Supercapacitor Electrodes, *Carbon*, 2009, **47**, p 1715–1722
20. C.L. Liu, W.S. Dong, G.P. Cao et al., Influence of KOH Followed by Oxidation Pretreatment on the Electrochemical Performance of Phenolic Based Activated Carbon Fibers, *J. Electroanal. Chem.*, 2007, **611**, p 225–231
21. D.W. Wang, F. Li, H.-T. Fang, M. Liu, and G.Q. Lu, Effect of Pore Packing Defects in 2-D Ordered Mesoporous Carbons in Ionic Transport, *J. Phys. Chem. B*, 2006, **110**, p 8570–8575
22. R. Lin, P.L. Taberna, J. Chmiola, D. Guay, Y. Gogosti, and P. Simon, Microelectrode Study of Pore Size, Ion Size, and Solvent Effects on the Charge/Discharge Behavior of Microporous Carbons for Electrical Double-Layer Capacitors, *J. Electrochem. Soc.*, 2009, **156**, p A7–A12